AIAA 81-4201

Singularities in Three-Dimensional Turbulent Boundary-Layer Calculations and Separation Phenomena

J. Cousteix*
Office National d'Etudes et de Recherches Aérospatiales (ONERA), Châtillon, France
and
R. Houdeville*
Centre d'Etudes et de Recherches de Toulouse, Toulouse, France

The possibility of the occurrence of singularities in three-dimensional turbulent boundary-layer calculations in the direct mode is studied here. For this, the system of the entrainment and global momentum equations is used and it is shown that the system is totally hyperbolic. It is demonstrated that singularities can be formed by focusing of the wall streamlines which are also characteristic lines of the system of equations. It should be emphasized that such a wall streamline configuration should not be confused with the separation phenomenon. An analogy is established with the unsteady two-dimensional case for which singularities are also formed by focusing of the characteristic lines. The singularities are avoided in the inverse mode. The formulation and implementation of the method are presented and an application to an experimental case with separation is discussed.

I. Introduction

THE determination of separated regions in three-dimensional flows on regular surfaces is linked to the topology of the wall streamlines. In order to determine them, the most convenient theoretical means is to calculate the boundary layer. In a classic way, such a calculation consists of determining the boundary-layer development from a prescribed external flow. However, in the simplest case of a two-dimensional flow, such a technique leads to a singularity at the zero skin-friction point. The practical effect of this singularity is to produce physically unrealistic solutions in which the derivatives of certain boundary-layer characteristics become infinite.

In three-dimensional flow, the existing analyses tend to prove that singularities can also occur but their structure is not as well understood as in the two-dimensional case. Moreover, several authors have confused numerical breakdowns with real separation lines and a lot of misunderstanding has resulted. Actually, a separation line must have properties of regularity[1] and should not be confused with a singularity line.

Several authors claim that the difficulty arises from an improper use of the boundary-layer equations that would no longer be valid near separation. Such a conclusion seems to be wrong, because, in the two-dimensional case, it has been demonstrated that the singularities are avoided by using the so-called inverse methods.[2-5] It must be remembered that in the direct mode the external velocity is prescribed, whereas in the inverse mode the external velocity is an unknown and boundary-layer parameters, as, for example, the displacement thickness or the skin-friction, become data. It is logical to think that things are similar for the three-dimensional case. Then, there is no reason for the wall streamlines to be singular near and along a separation line.

In order to analyze the listed problems correctly, it is important to know the conditions under which singularities can occur in the direct formulation of a boundary-layer calculation procedure. It is also important to define the nature of these singularities.

Received July 7, 1980; revision received Jan. 8, 1981.

*Research Engineer.

The present study has yet another aspect. In the two-dimensional case, it is known that the singularities have effects upstream of them although they have a local character; in effect, near a singular point, the solution becomes sensitive to a lot of parameters like, for example, the numerical approximation. Then, it would be misleading, when analyzing calculation models, to confuse modeling inaccuracies with difficulties due to the proximity of singularities.

To avoid the singularities and the subsequent difficulties, it is interesting to proceed in an inverse mode. This method can be used profitably in the following flow situations, though they do not constitute an exhaustive list.

1) The inverse mode can be used near the separation region or in zones including separated flows, when one wishes to adjust a calculation model by comparing the results of the computation with those of an experiment. In this case, the experiment must include boundary-layer measurements which are used as data in the calculation. Then the calculated and experimental characteristics of the external flow are compared.

2) It can be used when viscous and inviscid flowfields are solved simultaneously.

3) It can be used in design problems: starting with certain prescribed boundary-layer parameters it is possible to obtain the external velocity distribution by an inverse method applied to boundary-layer equations; subsequent application of the inverse method to Euler's equations give the airfoil coordinates.

4) It can be used in an iterative calculation with an optimization of the boundary-layer characteristics[6] in order to approach, as closely as possible, a prescribed external flow by rejecting all solutions with singularity; in fact, the difficulty consists in defining precisely the meaning of "as closely as possible."

All the formerly mentioned problems, viz., analysis of singularities in the direct mode, elaboration of an inverse method, etc., will be examined for turbulent flow by means of an integral method. The study is similar to the one carried out in unsteady two-dimensional flow.[7,8]

The analysis being performed with global equations is not exactly identical to the solution of the local equations, since the method is based on a set of closure relationships. However, the accuracy of the results is good both regarding the comparisons with experiment and the mathematical

behavior. For instance, the features of singularity in two-dimensional flow compare well with those of the Goldstein singularity. Therefore, we believe that a high level of similarity with the local equations can be attributed to the global equations, taking into account the adopted relationships.

II. Analysis of the Direct Mode

The integral method for three-dimensional turbulent boundary layers uses the entrainment and global momentum equations. In Ref. 9, the equations are presented in a general coordinate system with arbitrary metric coefficients. However, the properties of these equations are clearer if streamline coordinates are used because the closure relationships have been established in such an axis system. The x axis coincides with the projection on the wall of the external streamline and the z axis is orthogonal to the streamline in a plane tangent to the wall, the y axis being orthogonal to the wall.

Equations

Before writing the global boundary-layer equations, let us specify the notations.

In these equations, $\partial/\partial s$ and $\partial/\partial n$ represent the derivatives $(1/h_1)(\partial/\partial x)$ and $(1/h_2)(\partial/\partial z)$ where x and z are the generalized coordinates defined in the streamwise and crosswise directions; h_1 and h_2 are the associated metric coefficients. K_2 and K_1, the geodesic curvatures of the x and z lines, are related to the metric coefficients by the formulas

$$K_1 = -\frac{1}{h_1 h_2}\frac{\partial h_2}{\partial x} \qquad K_2 = -\frac{1}{h_1 h_2}\frac{\partial h_1}{\partial z}$$

If the external flow is isenthalpic and free of shock, we have

$$V_e \times \text{curl } V_e = 0$$

Hence the vector curl V_e is either zero or parallel to V_e. In both cases, its component along y is zero. In the streamline coordinates, we get

$$-\frac{1}{h_1 h_2}\frac{\partial}{\partial z} h_1 u_e = 0$$

and thus

$$K_2 = \frac{1}{u_e h_2}\frac{\partial u_e}{\partial z}$$

Let u and w be the streamwise and crosswise components of the velocity in the boundary layer. We define the following integral thicknesses which are contained in the global equations:

$$\delta_1 = \int_0^\delta (1-u/u_e)\,dy \qquad \theta_{11} = \int_0^\delta u/u_e(1-u/u_e)\,dy \qquad H = \delta_1/\theta_{11}$$

$$\delta_2 = \int_0^\delta -w/u_e dy \qquad \theta_{22} = \int_0^\delta -w^2/u_e^2 dy$$

$$\theta_{21} = \int_0^\delta -wu/u_e^2 dy \qquad \theta_{12} = \int_0^\delta w/u_e(1-u/u_e)\,dy$$

where δ is the boundary-layer thickness. C_{fs} and C_{fn} are the skin-friction coefficient components

$$\frac{C_{fs}}{2} = \frac{\tau_{ws}}{\rho_e u_e^2} \qquad \frac{C_{fn}}{2} = \frac{\tau_{wn}}{\rho_e u_e^2}$$

We also define the angle β_0 between the limiting wall streamline and the external streamline

$$\tan\beta_0 = \lim_{y\to 0}\frac{w}{u} = \frac{C_{fn}}{C_{fs}}$$

For an incompressible flow, the streamwise and crosswise global equations of momentum, and the entrainment equation are[10]

$$\frac{C_{fs}}{2} = \frac{\partial\theta_{11}}{\partial s} + \theta_{11}\left(\frac{H+2}{u_e}\frac{\partial u_e}{\partial s} - K_1\right) + \frac{\partial\theta_{12}}{\partial n} + \theta_{12}\left(\frac{2}{u_e}\frac{\partial u_e}{\partial n} - 2K_2\right) + \delta_2\left(\frac{1}{u_e}\frac{\partial u_e}{\partial n} - K_2\right) + K_1\theta_{22} \tag{1}$$

$$\frac{C_{fn}}{2} = \frac{\partial\theta_{21}}{\partial s} + \theta_{21}\left(\frac{2}{u_e}\frac{\partial u_e}{\partial s} - 2K_1\right) + K_2\theta_{11}(H+1) + \frac{\partial\theta_{22}}{\partial n} + \theta_{22}\left(\frac{2}{u_e}\frac{\partial u_e}{\partial n} - K_2\right) \tag{2}$$

$$\frac{\partial\delta}{\partial s} - \frac{v_e}{u_e} = \frac{\partial(\delta-\delta_1)}{\partial s} + (\delta-\delta_1)\left(\frac{1}{u_e}\frac{\partial u_e}{\partial s} - K_1\right) - \frac{\partial\delta_2}{\partial n} - \delta_2\left(\frac{1}{u_e}\frac{\partial u_e}{\partial n} - K_2\right) \tag{3}$$

Closure Relationships

The three global equations [Eqs. (1-3)] contain the following ten unknowns: the thicknesses δ, δ_1, δ_2, θ_{11}, θ_{21}, θ_{12}, θ_{22}; the skin-friction coefficient components C_{fs}, C_{fn}; and the entrainment coefficient $C_E = (\partial\delta/\partial s) - (v_e/u_e)$. From the definition of θ_{12}, δ_2, and θ_{21}, we have only one additional relationship

$$\theta_{12} + \delta_2 = \theta_{21}$$

Therefore, it is necessary to add hypotheses to arrive at a closed system. To this end, we have used similarity solutions,[9] the analysis of which leads to a set of closure relationships which depend on the three following parameters:

$$G = \frac{H-1}{H\sqrt{C_{fs}/2}} \qquad \Re_{\theta_{11}} = \frac{\rho_e u_e \theta_{11}}{\mu_e} \qquad T = -\frac{\delta_2/\delta}{K_2\delta}$$

These full closure relationships are not necessary for the present purpose and hence are not reproduced here; they are discussed extensively in Ref. 9. We will rather use approximations for high enough values of G corresponding to mild or strong positive streamwise pressure gradients. Though not sufficient for an accurate calculation, they are acceptable for the present analysis. Such a procedure has been adopted to simplify the algebra.

An important relationship expresses the factor $H^* = (\delta-\delta_1)/\theta_{11}$ as a function of the shape parameter $H = \delta_1/\theta_{11}$. The similarity solutions show that H^* is also a function of the Reynolds number $\Re_{\theta_{11}}$, but this effect is negligible for positive streamwise pressure gradients. The simplified form of this relationship is written as follows:

$$H^* = \frac{\delta-\delta_1}{\theta_{11}} = \frac{\alpha H^2 + H}{H-1} \qquad (\alpha = 0.631) \tag{4}$$

Moreover, the relationships between the crosswise thicknesses are expressed by means of an additional unknown C which

will be defined later

$$\frac{\delta_2}{\theta_{11}} = -CH \qquad \frac{\theta_{12}}{\theta_{11}} = C(H-1)$$

$$\frac{\theta_{21}}{\theta_{11}} = -C \qquad \frac{\theta_{22}}{\theta_{11}} = -C^2(H-1) \tag{5}$$

Hypotheses (5) are equivalent to assuming that, in the hodograph plane the profile $w(u)$ is linear in the external region of the boundary layer with a slope C

$$\frac{w}{u_e} = C\left(1 - \frac{u}{u_e}\right)$$

Although the rule is not general, the polar plot often appears as indicated in Fig. 1. Obviously, the hypothesis of linearity is wrong near the wall because of the no-slip condition, but the concerned region is very thin even if the maximum of w corresponds to values of u/u_e in the range 0.5-0.6. Then, the resulting error in the estimated thicknesses is negligible and unlikely to affect the analysis.

For an actual boundary-layer calculation, additional relationships for C_E, C_{fs}, and C_{fn} are necessary. However, they do not play any role in the study of the properties of the global equations as they do not involve derivatives of boundary-layer parameters. It is, therefore, not useful to give them here.

Nature of the System of Equations

Taking into account the proposed closure relationships, only three main unknowns are present in the global Eqs. (1-3). Their choice is arbitrary and we have adopted δ_1, θ_{11}, and C. With these functions, Eqs. (1-3) become

$$\frac{\partial \theta_{11}}{\partial s} - C\frac{\partial \theta_{11}}{\partial n} + C\frac{\partial \delta_1}{\partial n} + (\delta_1 - \theta_{11})\frac{\partial C}{\partial n} = A_1 \tag{6}$$

$$-C\frac{\partial \theta_{11}}{\partial s} + C^2\frac{\partial \theta_{11}}{\partial n} - C^2\frac{\partial \delta_1}{\partial n} - \theta_{11}\frac{\partial C}{\partial s} - 2C(\delta_1 - \theta_{11})\frac{\partial C}{\partial n} = A_2 \tag{7}$$

$$(H^* - HH^{*\prime})\frac{\partial \theta_{11}}{\partial s} + H^{*\prime}\frac{\partial \delta_1}{\partial s} + C\frac{\partial \delta_1}{\partial n} + \delta_1\frac{\partial C}{\partial n} = A_3 \tag{8}$$

with

$$H^{*\prime} = \frac{dH^*}{dH}$$

and

$$A_1 = \frac{C_{fs}}{2} - \theta_{11}\left(\frac{H+2}{u_e}\frac{\partial u_e}{\partial s} - K_1\right) - K_1\theta_{22}$$

$$A_2 = \frac{C_{fn}}{2} - \theta_{21}\left(\frac{2}{u_e}\frac{\partial u_e}{\partial s} - 2K_1\right) - K_2\theta_{11}(H+1) - \frac{\theta_{22}}{u_e}\frac{\partial u_e}{\partial n}$$

$$A_3 = C_E - (\delta - \delta_1)\left(\frac{1}{u_e}\frac{\partial u_e}{\partial s} - K_1\right)$$

Equations (6-8) constitute a system of first-order linear partial-differential equations, the nature of which is studied by means of the characteristic equation. It must be noted that C_{fs}, C_{fn}, and C_E are included in the right-hand side of Eqs. (6-8).

Let $1/\lambda$ be the slope of a characteristic line in the earlier defined external streamline axis system. So, the angle between a characteristic line and the external streamline is $\tan^{-1}(1/\lambda)$.

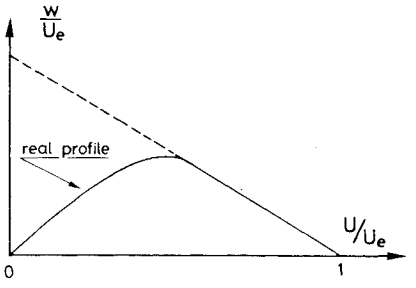

Fig. 1 Simplified polar plot.

Here, λ is the solution of the following characteristic equation:

$$C^3\lambda^3 - C^2\lambda^2\left(\frac{(H-1)(H^* - HH^{*\prime} + H^{*\prime} - 1) + 1}{H-1}\right)$$

$$+ C\lambda\left(\frac{H^* - 2HH^{*\prime} + 2H^{*\prime} - 1}{H-1}\right) + \frac{H^{*\prime}}{H-1} = 0$$

With the help of the relationship Eq. (4), the coefficients of this equation can be expressed as functions of H alone. We get

$$C^3\lambda^3 - C^2\lambda^2\frac{(2\alpha H+3)}{H-1} + C\lambda\frac{(-\alpha H^2 + 4\alpha H + 3)}{(H-1)^2}$$

$$+ \frac{\alpha H^2 - 2\alpha H - 1}{(H-1)^3} = 0 \tag{9}$$

It is easy to verify that a root of the preceding equation is

$$C\lambda_1 = \frac{1 - \alpha_1 H}{H-1} \tag{10}$$

where α_1 is related to α through: $\alpha_1 = -\alpha + (\alpha^2 + \alpha)^{1/2}$ ($\alpha = 0.631$; $\alpha_1 = 0.383$).

Then the characteristic equation takes the form

$$\left(C\lambda - \frac{1 - \alpha_1 H}{H-1}\right)\left(C^2\lambda^2 - \frac{H(2\alpha + \alpha_1) + 2}{H-1}C\lambda\right.$$

$$\left. + \frac{(\alpha/\alpha_1)H + 1}{(H-1)^2}\right) = 0$$

The other two roots are

$$C\lambda_2 = \frac{1}{H-1} \tag{11}$$

$$C\lambda_3 = \frac{(2\alpha + \alpha_1)H + 1}{H-1} \tag{12}$$

This calculation of the roots of the characteristic equation leads to the following conclusion: since the roots are real and distinct, the set of global equations is totally hyperbolic. Qualitatively, these results are identical to those given by Myring[10] who has developed a similar analysis by using slightly different closure relationships.

Before discussing the consequences, it is worthwhile specifying the configuration of the three characteristic lines. Of particular importance is the root λ_1, for it defines a line which can be identified with the wall streamline.

We recall that β_0 is the angle between the wall streamline and the external streamline. Among the set of closure relationships deduced from the similarity solutions,[9] one

relationship enables us to calculate β_0. For high enough values of the Clauser parameter G, this relationship can be simplified and is expressed by[9]:

$$\tan\beta_0 = \frac{C(H-1)}{1-\gamma H} \tag{13}$$

where γ is a coefficient for which we have proposed the value $\gamma = 0.438$ (Ref. 9).

The wall streamline and the λ_1-characteristic line are identical if they form the same angle with the external streamline, i.e.,

$$\tan\beta_0 = 1/\lambda_1$$

Therefore, Eqs. (10) and (13) show that the identity is rigorous if $\alpha_1 = \gamma$. In fact, the values of α_1 and γ are close to each other and a slight adjustment of the previously proposed relationship for β_0 would be sufficient to arrive at complete agreement. The other two characteristic directions lie between the external streamline and the wall streamline as shown in Fig. 2.

The properties of the global equations were foreseeable intuitively. In effect, it has been shown that the set of the local boundary-layer equations (continuity and momentum equations) possesses a system of an infinity of sub-characteristic directions which are the boundary-layer streamlines.[11] The effect of working with integrated equations is to decrease the number of characteristic lines because the number of unknowns is smaller. This number depends on the number of global equations. We can imagine the use of additional equations, for example equations of moment of momentum up to any order. Then the number of characteristic lines would be increased in the same way as the number of unknowns. However, the main features of the flow are described correctly by using only three global equations. Particularly, it is important to have identified a characteristic line with the wall streamline; at the same time we underline the coherence of the proposed closure relationships.

Practical Considerations for the Integration of the Equations

The hyperbolicity of the set of global equations leads to the concept of domains of dependence and influence; it dictates the specifications of the boundary conditions in order to calculate the boundary layer in a prescribed domain. Briefly, it is sufficient to say that as many boundary conditions as characteristic lines which enter the domain of calculation are needed. Then, it is clear that a rule is found, equivalent to that which must be observed if the local equations are used.

Another important consequence of the hyperbolicity of the set of the global equations is the choice of a numerical scheme compatible with the characteristic directions. For example, the use of noncentered finite-difference approximations for the crosswise derivatives or the integration step in the case of certain explicit schemes must take into account the sign and the values of the roots λ_1, λ_2, λ_3.

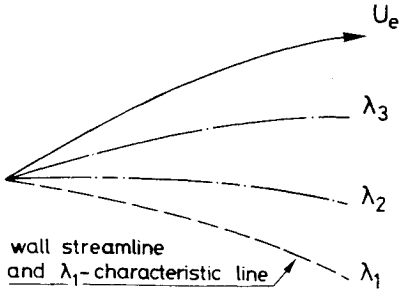

Fig. 2 Configuration of the characteristic lines; — external streamline, ——— λ_1-characteristic or wall streamline.

Singularities

In this section, we shall specify the conditions under which singularities can occur in a three-dimensional boundary-layer calculation in the direct mode. Before dealing with this problem, it is useful to recall briefly the results of the two-dimensional case in order to understand how they constitute a particular or degenerate form of the three-dimensional one.

The two-dimensional equations are obtained from Eqs. (6-8) by setting $C=0$. The crosswise momentum equation becomes trivial and the entrainment and streamwise momentum equations are written as

$$\frac{\partial\theta_{11}}{\partial s} = A_1' \tag{14}$$

$$(H^* - HH^{*\prime})\frac{\partial\theta_{11}}{\partial s} + H^{*\prime}\frac{\partial\delta_1}{\partial s} = A_3' \tag{15}$$

with

$$A_1' = \frac{C_{fs}}{2} - \theta_{11}\frac{H+2}{u_e}\frac{\partial u_e}{\partial s} \qquad A_3' = C_E - \frac{\delta-\delta_1}{u_e}\frac{\partial u_e}{\partial s}$$

Equations (14) and (15) constitute a system for two unknowns $(\partial\theta_{11}/\partial s)$ and $(\partial\delta_1/\partial s)$ the determination of which enables us to construct locally a solution from the initial data. Generally, a solution exists but a difficulty will arise if the determinant of the system Eqs. (14) and (15) is zero, i.e., if $H^{*\prime}=0$. In this case, the derivative $(\partial\delta_1/\partial s)$ will become infinite unless Eqs. (14) and (15) are compatible. The compatibility relation is $A_1' = A_3'/H^*$. In this hypothesis, the system is indeterminate but this eventuality is highly improbable if the boundary-layer equations are solved in the direct mode. So, at the point $H^{*\prime}=0$ the solution is such that $(\partial\delta_1/\partial s)$ is generally infinite which is not physically possible. Relationship Eq. (4) shows that this point corresponds to a critical value of the shape parameter around $H_c = 2.6$. Among the set of closure relationships of Eqs. (14) and (15), one relationship enables us to calculate C_{fs} (Ref. 12). It has been shown[12] that the condition $C_{fs}=0$ is obtained when $H = H_{Cf=0} \simeq 2.35$. In fact, a slight adjustment of the closure relationships would be sufficient to equalize the two values H_c and $H_{Cf=0}$ of the shape parameter. So, the integral method behaves in a way similar to the Goldstein singularity of the local equations.

In three-dimensional flow, there is no reason for the point $H^{*\prime}=0$ to be singular, in general. At such a point, the characteristic equation shows that there always exists three real, and distinct, characteristic values. The passage through a point $H^{*\prime}=0$ implies only the incipient occurrence of an influence from downstream to upstream because the wall streamline becomes orthogonal to the external streamline (Fig. 3).

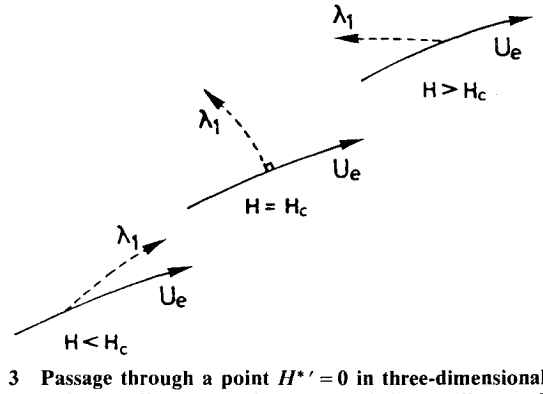

Fig. 3 Passage through a point $H^{*\prime}=0$ in three-dimensional flow; — external streamline, ——— λ_1-characteristic or wall streamline.

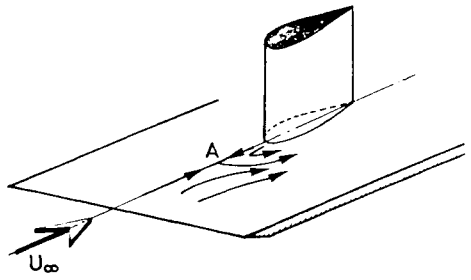

Fig. 4 Particular case in three-dimensional flow.

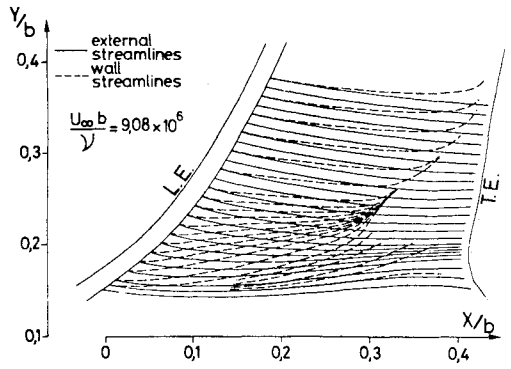

Fig. 5 Three-dimensional turbulent boundary layer; plot of the wall streamlines. Examples of calculation with singularities in the direct mode.

However, we can give a purely three-dimensional example in which the point $H^{*\prime}=0$ is singular. It is the flow over a flat plate on which a symmetric cylinder is set orthogonally (Fig. 4). The upstream velocity is parallel to the plate and to the plane of symmetry of the obstacle. Separation occurs in front of this obstacle, and from the plot of the wall streamlines a separation line can be defined which intersects the plane of symmetry orthogonally at the point A.

The flow in the plane of symmetry does not obey purely two-dimensional equations because they contain nonzero crosswise derivatives of the crossflow. Nevertheless, the equations show that the point A, where $H^{*\prime}=0$, ($C_{fs}\simeq 0$) is singular. In the immediate vicinity of this point, the wall streamline is orthogonal to the plane of symmetry and it is interesting to note that the proposed law for β_0 [Eq. (13)] accounts for this situation. In effect, Eq. (13) indicates that β_0 is equal to 90 deg if $H=1/\gamma$. The given value of γ ($\gamma=0.438$) leads to $H=2.28$. If we took $\alpha_1=\gamma=0.383$, the angle β_0 would be equal to 90 deg for $H=H_c=2.6$ ($H^{*\prime}=0$) and we would obtain a rigorous coherence.

Generally, in the three-dimensional case, the singularities are not local. They must be sought rather in configurations leading to a focusing of the characteristic lines belonging to the same family. More precisely, they are the lines defined by λ_1, i.e., the wall streamlines which are likely to focus. They may, then, possess an envelope that is not a wall streamline and that defines a physically meaningless singular line.

To emphasize such a phenomenon, we present an example of calculation in which it occurs. The basis is an experimental study by Lindhout et al.[13] This experiment has been used as a test case for a workshop on three-dimensional turbulent boundary layers held in Amsterdam (Sept. 1979[14]).

The objective was to calculate the boundary layer developing on a wing-root. The data consists of the magnitude and direction of the velocity in inviscid flow. Boundary-layer characteristics were given as initial data along a starting line close to the leading edge. The calculations were performed by using full closure relationships that are more accurate than those given by Eq. (4) and (5). The computed wall streamlines are shown in Fig. 5. This figure also shows the external streamlines and the contours of the leading and trailing edges.

The experimental results, based on wall flow visualizations, are in good agreement with the calculations except in the vicinity of the calculated singular line. In effect, the experiment indicates the existence of a three-dimensional separation but the separation line is not at all singular. Unless examined carefully, the calculated pattern of the wall streamlines near the singular line could be confused with the experimental pattern near the separation line. However, such an interpretation of the experiment would be wrong because the experimental separation line is regular. We shall come back to this later and show that the calculated singularity is physically meaningless.

Finally, in the domain ($x/b>0.3$; $z/b>0.2$) we note the fan shaped pattern of the wall streamlines. It is easy to imagine the existence of a dividing line which is also revealed by the experiment.

Analogy with the Unsteady Two-Dimensional Boundary Layer

To analyze the singular behavior of the equations thoroughly, it is helpful to compare the steady three-dimensional case with the unsteady two-dimensional case; an analogy exists between them.

First of all, we recall the results obtained in the unsteady case.[7] The basic equations are the entrainment equation and the global momentum equation. For an incompressible flow, they are

$$\frac{1}{u_e}\frac{\partial}{\partial x}u_e(\delta-\delta_1)=C_E \quad \text{with} \quad C_E=\frac{\partial\delta}{\partial x}-\frac{v_e}{u_e} \tag{16}$$

$$\frac{\partial\theta}{\partial x}+\theta\frac{H+2}{u_e}\frac{\partial u_e}{\partial x}+\frac{1}{u_e^2}\frac{\partial}{\partial t}\delta_1 u_e=\frac{C_f}{2} \tag{17}$$

Let us note that the steady two-dimensional Eqs. (14) and (15) are in fact a special case of the preceding equations.

This system involves five unknowns: C_E, C_f, δ_1, θ, and δ. The closure relationships have been obtained from similarity solutions extended to the unsteady case. They are a priori functions of two parameters, the Clauser parameter G and the Reynolds number $\mathcal{R}_{\theta_{11}}$. However, for positive pressure gradients these relationships can be simplified in order to facilitate the study of the properties of the equations. Particularly, in the relationship between $H^*=(\delta-\delta_1)/\theta$ and $H=\delta_1/\theta$, the influence of the Reynolds number becomes very small. This relationship is the same as that for the study of the three-dimensional case [Eq. (4)].

$$H^*=\frac{\alpha H^2+H}{H-1} \qquad \alpha=0.631$$

On the other hand, the similarity solutions have shown that the entrainment coefficient C_E is expressed as

$$C_E=C_{E_S}-\frac{1}{u_e}\frac{\partial\delta}{\partial t}$$

where C_{E_S} is the same algebraic function of G and $\mathcal{R}_\theta$ as in the steady case.

The functions C_{E_S}, as well as the skin friction law, do not play a role in the study of the properties of the global equations because they do not involve derivatives of boundary-layer parameters. Therefore, they are not given here.

With the aid of the previously given set of closure relationships the number of the main unknowns is reduced to

two. If we choose δ_1 and θ, the global equations will be

$$H^{*\prime}\frac{\partial \delta_1}{\partial x}+\frac{1+H^{*\prime}}{u_e}\frac{\partial \delta_1}{\partial t}+(H^*-HH^{*\prime})\frac{\partial \theta}{\partial x}$$

$$+\frac{H^*-HH^{*\prime}}{u_e}\frac{\partial \theta}{\partial t}=B_1 \tag{18}$$

$$\frac{1}{u_e}\frac{\partial \delta_1}{\partial t}+\frac{\partial \theta}{\partial x}=B_2 \tag{19}$$

with

$$B_1=C_{E_S}-\frac{\delta-\delta_1}{u_e}\frac{\partial u_e}{\partial x} \qquad B_2=\frac{C_f}{2}-\frac{\theta(H+2)}{u_e}\frac{\partial u_e}{\partial x}-\frac{\delta_1}{u_e^2}\frac{\partial u_e}{\partial t}$$

Equations (18) and (19) constitute a system of first-order partial-differential equations for δ_1 and θ. The characteristic equation is of the second order for the reduced quantity $\lambda=\mathrm{d}x/u_e\mathrm{d}t$; it is

$$\lambda^2(H^*-HH^{*\prime})+\lambda[1-H^*+H^{*\prime}(1+H)]-H^{*\prime}=0 \tag{20}$$

We can calculate the roots of Eq. (20) explicitly by using the simplified relationship $H^*(H)$

$$\lambda_1=[1+(H-1)\sqrt{\alpha/(1+\alpha)}]/H \tag{21}$$

$$\lambda_2=[1-(H-1)\sqrt{\alpha/(1+\alpha)}]/H \tag{22}$$

Therefore, in the domain $H>1$, the following conclusions can be drawn. 1) Since there are always two real, and distinct, characteristic directions, the system is hyperbolic. 2) One of the characteristic values (λ_1) is always positive. Moreover λ_1 is close to $1{:}0.62<\lambda_1<1$. 3) The other characteristic value (λ_2) is positive when $H<H_c$; λ_2 is negative when $H>H_c$. The point $H=H_c$ ($H_c\simeq 2.6$) is defined by the condition $H^{*\prime}=0$ and it can be identified with the point $C_f=0$.

Thus, the point $H=H_c$ is not generally a singular point in unsteady flow. The change of sign of λ_2 when H becomes greater than H_c is reflected by an influence from downstream to upstream. The meaning of this influence is very clear because it is related to the occurrence of reverse flows.

The characteristic line corresponding to λ_2 plays a key role in the definition of singularities. This role is very similar to that of the wall streamlines (which are also characteristic lines) in the three-dimensional case. We have shown, with the aid of various calculations,[7] that this characteristic family gives rise to a focusing in particular circumstances. The result is a line across which certain boundary-layer quantities are discontinuous.

An example of computed results is given in Fig. 6 where the two families of characteristic lines are drawn. The zero skin friction points are those for which the tangent to the λ_2-characteristic line is parallel to the time axis. It can be noted that these points are free of singularity. The characteristic lines converge for the higher values of time and finally form a discontinuity line. These results have been obtained with an integration scheme of the predictor-corrector type and have been confirmed by integrating the equations with the method of characteristics. The comparison of Figs. 5 and 6 shows a rather spectacular resemblance and there is undoubtedly a strong analogy between the two cases.

Obviously, the existence of a discontinuity line is not physically possible. Moreover, in the course of the formation of this line, the derivative of δ_1, for example, as well as the value of the velocity normal to the wall, becomes very large. Thus, one could think that the boundary-layer hypotheses themselves are no longer valid. However, as in the steady two-dimensional case, such a conclusion would be premature. In

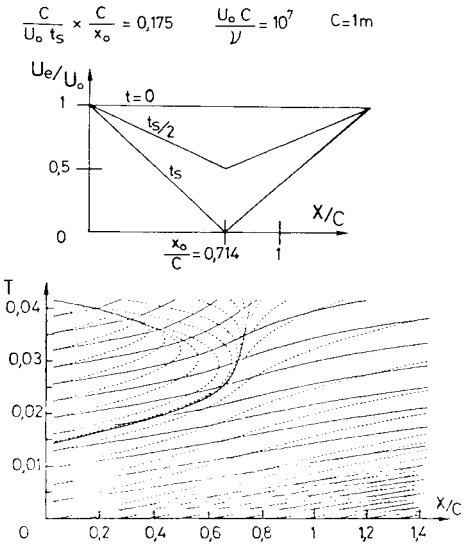

Fig. 6 Unsteady two-dimensional turbulent boundary layer. Plot of the characteristic lines ($-\lambda_1$---λ_2). Example of calculation with singularities in the direct mode.

effect, a similar situation is observed in two-dimensional flow when approaching the singular point $H=H_c$; the derivative of δ_1 increases until it is infinite at the point $H=H_c$. It is known that the difficulty is an inherent feature of the direct mode and that it is avoided by using an inverse method. We have also shown that, in unsteady flow, the inverse mode enables us to prevent the occurrence of any singularity.[8] In addition, it is probable that the formation of a discontinuity line is a signal that reveals that a strong coupling with the nonviscous flow is needed.

In the three-dimensional case, the convergence of the wall streamlines can also lead to a discontinuity line. Obviously such a discontinuity is physically meaningless. It is, once more, an intrinsic difficulty of the direct mode. As has been demonstrated in the unsteady two-dimensional case, it is thought that these difficulties are avoided in the inverse mode and that the validity of the boundary-layer equations is not necessarily questionable. We do not have an example of three-dimensional calculation displaying a discontinuity. However, we are going to show the possibility of this eventuality.

First of all, let us note that the boundary-layer equations can be written in a quasiconservation form that is a necessary condition for the existence of a weak solution. From Eqs. (1-3) we get

$$\frac{\partial \theta_{11}}{\partial s}+\frac{\partial \theta_{12}}{\partial n}=\frac{C_{fs}}{2}-\theta_{11}\left(\frac{H+2}{u_e}\frac{\partial u_e}{\partial s}-K_1\right)$$

$$-\theta_{12}\left(\frac{2}{u_e}\frac{\partial u_e}{\partial n}-2K_2\right)-\delta_2\left(\frac{1}{u_e}\frac{\partial u_e}{\partial n}-K_2\right)-K_1\theta_{22} \tag{23}$$

$$\frac{\partial \theta_{21}}{\partial s}+\frac{\partial \theta_{22}}{\partial n}=\frac{C_{fn}}{2}-\theta_{21}\left(\frac{2}{u_e}\frac{\partial u_e}{\partial s}-2K_1\right)-K_2\theta_{11}(H+1)$$

$$-\theta_{22}\left(\frac{2}{u_e}\frac{\partial u_e}{\partial n}-K_2\right) \tag{24}$$

$$\frac{\partial(\delta-\delta_1)}{\partial s}-\frac{\partial \delta_2}{\partial n}=C_E-(\delta-\delta_1)\left(\frac{1}{u_e}\frac{\partial u_e}{\partial s}-K_1\right)$$

$$+\delta_2\left(\frac{1}{u_e}\frac{\partial u_e}{\partial n}-K_2\right) \tag{25}$$

By using the simplified closure relationships [Eqs. (4) and (5)], the preceding equations are written as

$$\frac{\partial \theta_{11}}{\partial s} + \frac{\partial}{\partial n}\left[C\theta_{11}(H-1)\right] = C_1 \tag{26}$$

$$\frac{\partial}{\partial s}(-C\theta_{11}) + \frac{\partial}{\partial n}\left[-C^2\theta_{11}(H-1)\right] = C_2 \tag{27}$$

$$\frac{\partial}{\partial s}(\theta_{11}H^*) + \frac{\partial}{\partial n}(C\theta_{11}H) = C_3 \tag{28}$$

Let us assume that a discontinuity line exists and let σ be the angle between this line and the external streamline. Equations (26-28) involve the conservation of certain quantities through the discontinuity line. To express this, let us note the quantities on each side of the discontinuity line by the subscripts a and b. We get

$$[\theta_{11}\sin\sigma - C\theta_{11}(H-1)\cos\sigma]_a = [\theta_{11}\sin\sigma - C\theta_{11}(H-1)\cos\sigma]_b \tag{29}$$

$$[C\theta_{11}\sin\sigma - C^2\theta_{11}(H-1)\cos\sigma]_a = [C\theta_{11}\sin\sigma - C^2\theta_{11}(H-1)\cos\sigma]_b \tag{30}$$

$$[\theta_{11}H^*\sin\sigma - C\theta_{11}H\cos\sigma]_a = [\theta_{11}H^*\sin\sigma - C\theta_{11}H\cos\sigma]_b \tag{31}$$

Dividing member by member Eqs. (29) and (30) on the one hand and Eqs. (29) and (31) on the other, we get

$$C_a = C_b \tag{32}$$

$$\left[\frac{H^*\sin\sigma - CH\cos\sigma}{\sin\sigma - C(H-1)\cos\sigma}\right]_a = \left[\frac{H^*\sin\sigma - CH\cos\sigma}{\sin\sigma - C(H-1)\cos\sigma}\right]_b \tag{33}$$

If the values H_a, C_a, and σ are assumed to be known, Eq. (33) is an equation for H_b. Taking into account the relationship Eq. (4), this equation is of the second order for H_b. Now, at least one root exists since $H_b = H_a$ is a solution. In general, a second distinct root exists and a discontinuous solution is thus possible.

III. Development of an Inverse Method for Three-Dimensional Turbulent Boundary Layers

A great variety of inverse methods can be invented according to the choice of the prescribed functions. However, we must bear in mind that one of the ultimate objectives is the inclusion of the inverse method in a coupling technique. In order not to deviate too much from this line, it is worthwhile examining a few possible solutions which are compatible with this aim.

Matching Equation, Displacement Thickness

A coupling method consists of calculating the viscous and inviscid flows simultaneously by imposing matching conditions between them. Two conditions are needed, one for the velocity parallel to the wall and the other for the transverse velocity. As a first approximation, the first condition is that the inviscid velocity at the wall is equal to boundary-layer edge velocity parallel to the wall. However, let us note that better approximations can be used.[2] The second condition concerns the velocity normal to the wall or, equivalently, the direction of the velocity vector with respect to the wall. To get this condition, it is shown later that the entrainment equation is combined with an expansion of the inviscid flow within the boundary layer determined by means of the local continuity equation written for the inviscid flow. Such a method is approximative[2] but sufficient for our purpose.

Generally, one needs to work in an arbitrary axis system. Let ξ and ζ be the coordinates parallel to the surface and y the perpendicular axis. Furthermore, μ_1 and μ_2 are the metric elements in the ξ and ζ directions. The metric element in the y direction can be taken as 1 according to the boundary-layer hypotheses. λ is the angle between the ξ and ζ axes. U_1 and W_1 are the external velocity components in the ξ and ζ directions. In this system, the local continuity equation is

$$q\frac{\partial \rho}{\partial t} + \frac{\partial}{\partial \xi}\left(\frac{q}{\mu_1}\rho U\right) + \frac{\partial}{\partial \zeta}\left(\frac{q}{\mu_2}\rho W\right) + q\frac{\partial}{\partial y}\rho v = 0, \quad q = \mu_1\mu_2\sin\lambda \tag{34}$$

With Eq. (34) and a Taylor series expansion, the external flow is extended within the boundary layer. If the wall curvatures are small enough with respect to the boundary-layer thickness, we can assume that, for the extended flow, the density and the streamwise velocity are constant and equal to their values, ρ_e and u_e, respectively, at the edge of the boundary layer. For the extended flow, let $\bar{v}_y$ be the velocity normal to the wall at any point y. A Taylor series expansion of $\bar{v}$ around $y = \delta$ gives

$$\bar{v}_y = \bar{v}_\delta + (y-\delta)\left(\frac{\partial \bar{v}}{\partial y}\right)_{y=\delta}$$

The term $(\partial\bar{v}/\partial y)_{y=\delta}$ can be expressed from Eq. (34) and we get

$$\frac{\bar{v}_y}{u_e} = \frac{\bar{v}_\delta}{u_e} - (y-\delta)\left[\frac{1}{\rho_e u_e q}\frac{\partial}{\partial \xi}\left(\frac{q\rho_e U_1}{\mu_1}\right) + \frac{1}{\rho_e u_e q}\frac{\partial}{\partial \zeta}\left(\frac{q\rho_e W_1}{\mu_2}\right) + \frac{1}{\rho_e u_e}\frac{\partial \rho_e}{\partial t}\right] \tag{35}$$

At the edge of the boundary layer, the velocity $\bar{v}_\delta$ is also equal to the velocity obtained from the entrainment equation. This equation is

$$\frac{v_\delta}{u_e} = \frac{U_1}{u_e\mu_1}\frac{\partial \delta}{\partial \xi} + \frac{W_1}{u_e\mu_2}\frac{\partial \delta}{\partial \zeta} - \frac{1}{\rho_e u_e q}\left[\frac{\partial}{\partial \xi}\left(\frac{\rho_e q}{\mu_1}(U_1\delta - u_e\Delta_1)\right) + \frac{\partial}{\partial \zeta}\left(\frac{\rho_e q}{\mu_2}(W_1\delta - u_e\Delta_2)\right)\right] + \frac{1}{\rho_e u_e}\frac{\partial}{\partial t}\rho_e(\delta_\rho - \delta) + \frac{1}{u_e}\frac{\partial \delta}{\partial t} \tag{36}$$

with

$$\Delta_1 = \int_0^\delta \frac{\rho_e U_1 - \rho U}{\rho_e u_e}\,dy \qquad \Delta_2 = \int_0^\delta \frac{\rho_e W_1 - \rho W}{\rho_e u_e}\,dy$$

$$\delta_\rho = \int_0^\delta \left(1 - \frac{\rho}{\rho_e}\right)dy$$

The matching equation is obtained by combining Eqs. (35) and (36). The matching point must now be specified, i.e., the value of y. Let us examine two cases: 1) $y = \delta^*$ where δ^* is the displacement thickness, and 2) $y = 0$, coupling at the wall.

In the first hypothesis, we need to define the displacement thickness. Lighthill[15] has proposed several interpretations that lead to the same definition but the formulation has been given in a streamline coordinate system. The generalization to an arbitrary axis system in unsteady flow results in the following differential equation for defining δ^*:

$$\frac{1}{q}\frac{\partial}{\partial \xi}\left(\frac{\rho_e q}{\mu_1}(\delta^* U_1 - \Delta_1 u_e)\right) + \frac{1}{q}\frac{\partial}{\partial \zeta}\left(\frac{\rho_e q}{\mu_2}(\delta^* W_1 - \Delta_2 u_e)\right) + \delta^*\frac{\partial \rho_e}{\partial t} - \frac{\partial}{\partial t}(\rho_e\delta_\rho) = 0 \tag{37}$$

Thus, the matching equation written at $y=\delta^*$ is

$$\frac{\bar{v}_{\delta^*}}{u_e}=\frac{U_1}{u_e\mu_1}\frac{\partial\delta^*}{\partial\xi}+\frac{W_1}{u_e\mu_2}\frac{\partial\delta^*}{\partial\zeta} \tag{38}$$

If x and z are the axes of a streamline coordinate system and h_1 and h_2 the corresponding metric elements, Eq. (38) can be written as

$$\frac{\bar{v}_{\delta^*}}{u_e}=\frac{\partial\delta^*}{h_1\partial x} \tag{39}$$

This equation shows that the displacement surface is an impermeable wall for the inviscid flow.

The second case, coupling at the wall, can be interpreted rather as a wall transpiration condition given by

$$\frac{\bar{v}_0}{u_e}=\frac{1}{\rho_e u_e q}\frac{\partial}{\partial\xi}\left(\frac{\rho_e u_e q\Delta_1}{\mu_1}\right)+\frac{1}{\rho_e u_e q}\frac{\partial}{\partial\zeta}\left(\frac{\rho_e u_e q\Delta_2}{\mu_2}\right)$$
$$+\frac{1}{\rho_e u_e}\frac{\partial}{\partial t}(\rho_e\delta_\rho) \tag{40}$$

In most of the applications the two matching conditions [Eq. (39) or (40)] should lead to nearly equivalent numerical results. However, the numerical treatment of the inviscid boundary condition is not the same. In the first case the displacement surface is a streamsurface, whereas in the second case we have a transpiration condition at the wall.

The examination of the two coupling possibilities shows that the thicknesses δ_1 and δ_2 play a key role. Let us note, however, that it is not equivalent to prescribing the distributions $\delta_1(x,z)$ and $\delta_2(x,z)$ or simply that of $\bar{v}_{\delta^*}(x,z)$ or $\bar{v}_0(x,z)$. Nevertheless, the construction of the inverse method is easier if the distributions of $\delta_1(x,z)$ and $\delta_2(x,z)$ are given. We have opted for this because our present aim is not to construct a coupling method but, more simply, to obtain a calculation code to control certain hypotheses or closure relationships in separated regions.

Proposed Method and Application

A three-dimensional separation does not necessarily involve streamwise reversed flow, but the direct mode becoming singular, it is necessary to use the inverse mode to study a separated zone even without reversed flow. When no negative streamwise velocity exists, there is no reason for the previously proposed closure relationships[9] to be not applicable although they have not been studied for separated regions. At the present time our closure relationships are limited by the point $C_{fs}=0$. Since the application case is within this framework, we have simply used the existing relationships.

We have tried to analyze the system of equations in the inverse mode in the same way as in the direct mode. The equations are those of entrainment and global momentum Eqs. (1-3), the prescribed functions are $\delta_1(x,z)$ and $\delta_2(x,z)$, and the main unknowns are the momentum thickness θ_{11} and the two components of the external velocity. To study the properties of the set of equations we form the characteristic equation again. Obviously, this equation is different from the one corresponding to the direct mode since the unknowns have been changed. We are led to a third-order equation which seems difficult to study analytically and we shall not give general conclusions.

We shall restrict ourselves to the presentation of the results obtained for the computed application case. This case (Fig. 7) is an experiment on a boundary layer developing over an "infinite swept wing."[16] Actually, the boundary layer is studied on a swept flat plate with a pressure distribution induced on it by a suitably shaped body near the plate. Very detailed boundary-layer measurements are available: mean

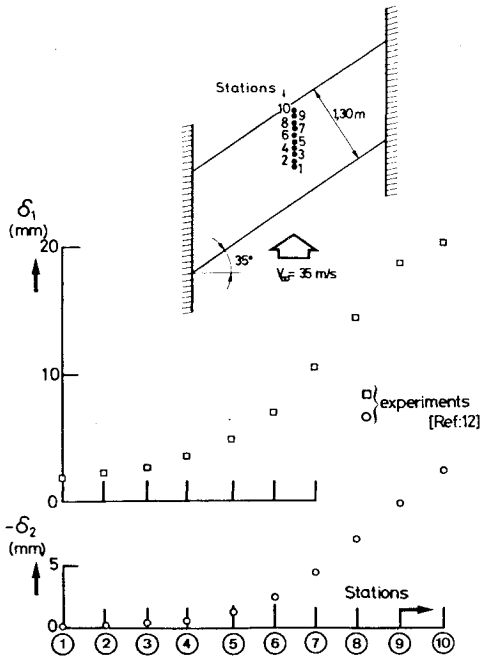

Fig. 7 Three-dimensional turbulent boundary layer; application of the inverse method; calculation data.

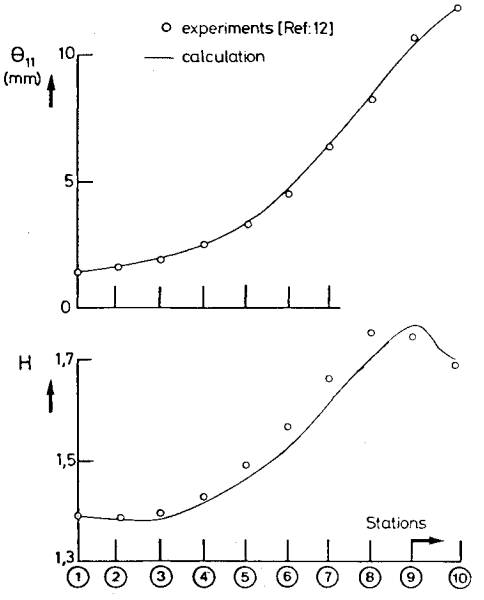

Fig. 8 Three-dimensional turbulent boundary layer; application of the inverse method; comparison with the experiment of θ_{11} and H.

velocity profiles at stations 1-10 (Fig. 7) and profiles of the six components of the Reynolds stress tensor at stations 4, 5, 7, 9, and 10. As indicated by the results, we can assume with a good approximation that the flow does not vary along the direction parallel to the leading edge.

Although two boundary-layer thicknesses δ_1 and δ_2 (Fig. 7), are used as given data, the comparison with the other experimental boundary-layer parameters is not irrelevant. Indeed, all the boundary-layer parameters cannot be derived from two of them because the closure relationships keep three parameters independent. Thus, it is worthwhile comparing the boundary-layer parameters other than δ_1 and δ_2 in order to control the closure relationships.

Figures 8-10 show that the agreement between calculation and experiment is excellent except, perhaps, for the skin-friction coefficient. It can be seen that the agreement is observed even near the separation line located between stations 8 and 9. In the case of an infinite swept wing, the separation line

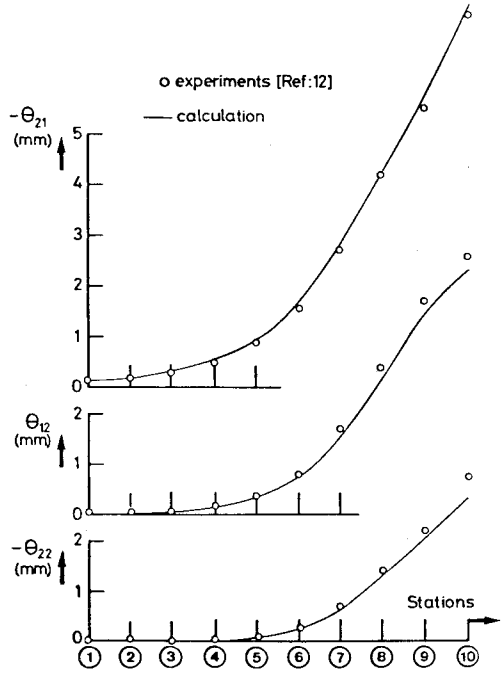

Fig. 9 Three-dimensional turbulent boundary layer; application of the inverse method; comparison with the experiment of θ_{21}, θ_{12} and θ_{22}.

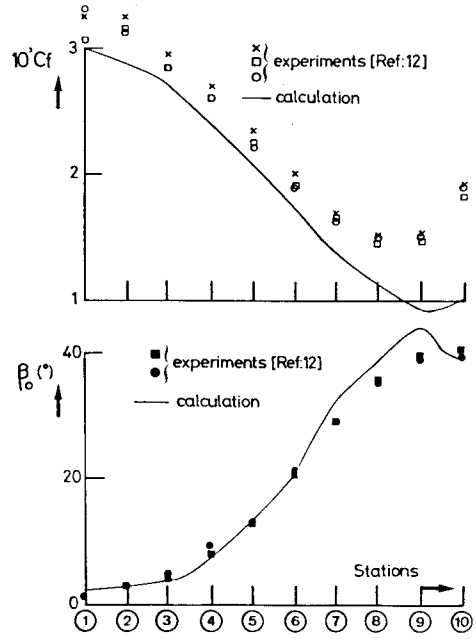

Fig. 10 Three-dimensional turbulent boundary layer; application of the inverse method; comparison with the experiment of c_f and β_0.

is observed when the wall streamlines become parallel to the leading edge. If α is the direction of the external streamline with respect to a line normal to the leading edge, this condition will be $\alpha+\beta_0=90$ deg. It should be noted that a singularity would occur in a calculation in the direct mode if this condition were fulfilled. In the inverse mode, the result is different since no singularity is noted along the separation line: the wall streamlines tend asymptotically toward the separation line.

Figure 11 gives the comparisons of the modulus of the external velocity and of its angle α with respect to a line normal to the leading edge. The hypothesis of infinite swept wing implies that the component of the external velocity parallel to the leading edge is a constant. Although this

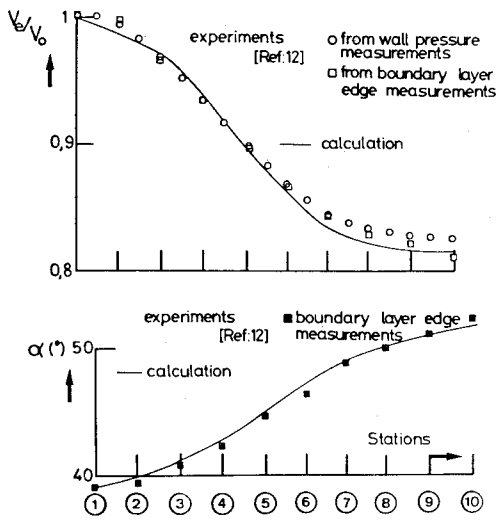

Fig. 11 Three-dimensional turbulent boundary layer; application of the inverse method; comparison with the experiment of the external flow.

condition is not introduced in the calculations, the results agree with it very well. The agreement obtained for the velocity modulus seems satisfactory, too. Obviously, it would be interesting to carry out such comparisons for other experimental cases in which the separated region would be more extended. Unfortunately, to our knowledge, such experiments with sufficiently detailed boundary-layer measurements are not available.

IV. Conclusions

The analysis of the properties of a system of global boundary-layer equations has shown the eventuality of the occurrence of singularities in calculations in the direct mode.

In the steady two-dimensional case, the singularity is defined by zero skin friction and is reflected by infinite values of the derivatives of certain boundary-layer parameters. In fact, it is a degenerate form of the singularities that can occur in the steady three-dimensional case or in the unsteady two-dimensional case. In these latter two cases, the point $C_f=0$ is no longer the signal of a singularity; this point simply indicates a change in the orientation of the boundaries of the domains of influence and of dependence.

In the steady three-dimensional or unsteady two-dimensional cases, the hyperbolicity of the equations and the existence of weak solutions can lead to discontinuous solutions. Therefore, a strong analogy exists between the two cases. However, we have been able to give a physical meaning only in the three-dimensional case to the characteristic lines that are the source of difficulties; with a few minor hypotheses, it has been shown that the characteristic line, which is likely to lead to singularities, is identifiable with a wall streamline.

In all the cases, the singularities lead to physically meaningless configurations and it would be wrong to interpret them as separation schemes, particularly in the three-dimensional case. However, these difficulties are not an argument for claiming that the boundary-layer equations are no longer valid in the vicinity of separation. By using inverse methods, we restore to the singular configurations of the direct mode the features of regularity which are physically needed.

References

[1] Legendre, R., "Lignes de courant d'un écoulement permanent. Décollement et séparation," *La Recherche Aérospatiale*, Nov.-Dec. 1977, pp. 327-335; English translation ESA TT 476.

[2] Le Balleur, J. C., "Couplage visqueux-non visqueux. Analyse du probléme incluant décollements et ondes de choc," *La Recherche Aérospatiale*, Nov.-Dec. 1977, pp. 349-358; English translation ESA TT 476.

[3] Catherall, D. and Mangler, K. W., "The Integration of Two-Dimensional Laminar Boundary-Layer Equations Past the Point of Vanishing Skin Friction," *Journal of Fluid Mechanics*, Vol. 26, Pt. 1, Sept. 1966, pp. 163-182.

[4] Klineberg, J. N. and Steger, J. L., "On Laminar Boundary-Layer Separation," AIAA Paper 74-94, Washington, Jan.-Feb. 1974.

[5] Carter, J. E., "Inverse Solutions for Laminar Boundary-Layer Flows with Separation and Reattachment," NASA TR-R-447, Nov. 1975.

[6] Arieli, R. and Murphy, J. D., "Pseudo-Direct Solutions to the Boundary-Layer Equation for Separated Flow," 17th Aerospace Sciences Meeting, New Orleans, 1979.

[7] Cousteix, J., Houdeville, R., and Desopper, A., "Résultats expérimentaux et méthodes de calcul relatifs aux couches limites turbulentes en écoulement instationnaire," AGARD Conference on Unsteady Aerodynamics, CP 227, 1977.

[8] Cousteix, J., Le Balleur, J. C., and Houdeville, R., "Calcul de couche limite instationnaire en modes direct ou inverse," *La Recherche Aérospatiale*, May-June 1980, pp. 147-157; English edition available.

[9] Cousteix, J., "Analyse théorique et moyens de prévision de la couche limite turbulente tridimensionnelle," ONERA 157, 1974; English translation ESA TT-238.

[10] Myring, D. F., "An Integral Prediction Method for Three-Dimensional Turbulent Boundary-Layers in Incompressible Flow," RAE TR 70 147, 1970.

[11] Krause, E., "Numerical Treatment of Boundary-Layer Problems," AGARD Lecture Series 64 on Advances in Numerical Fluid Dynamics, 1973.

[12] Michel, R., Quemard, C., and Durant, R., "Application d'un schéma de longueur de mélange a l'étude des couches limites turbulentes d'équilibre," ONERA N.T. 154, 1969.

[13] Lindhout, J.P.F., Moek, G., De Boer, E., and Van Den Berg, B., "A Method for the Calculation of 3D Boundary-Layers on Practical Wing Configurations," The Joint ASME-CSME Applied Mechanics, Fluids Engineering and Bio-engineering Conference, Niagara Falls, N.Y., 1979.

[14] Lindhout, J.P.F., van den Berg, B., Elsenaar, A., "Comparison of Boundary-Layer Calculations for the Root Section of a Wing, The September 1979 Amsterdam Workshop Test Case," NLR MP 80028 U, 1981.

[15] Lighthill, M. J., "On Displacement Thickness," *Journal of Fluid Mechanics*, Vol. 4, 1958, pp. 383-392.

[16] Van Den Berg, B., Elsenar, A., Lindhout, J.P.F. and Wesseling, P., "Measurements in an Incompressible Three-Dimensional Turbulent Boundary-Layer, under Infinite Swept Wing Conditions, and Comparison with Theory," *Journal of Fluid Mechanics*, Vol. 70, July 1975, p. 127.